IEEE Access
Multidisciplinary ⋮ Rapid Review ⋮ Open Access Journal

Received May 12, 2021, accepted June 14, 2021, date of publication June 17, 2021, date of current version June 28, 2021.

Digital Object Identifier 10.1109/ACCESS.2021.3090245

A New Advanced Method for an Accurate Assessment of Harmonic and Supraharmonic Distortion in Power System Waveforms

GUIDO CARPINELLI[1], (Member, IEEE), ANTONIO BRACALE[2], (Senior Member, IEEE), PIETRO VARILONE[3], (Member, IEEE), TOMASZ SIKORSKI[4], (Member, IEEE), PAWEL KOSTYLA[4], AND ZBIGNIEW LEONOWICZ[4], (Senior Member, IEEE)

[1]Department of Electrical Engineering and Information Technology, University of Naples Federico II, 80125 Naples, Italy *(Retired)*
[2]Department of Engineering, University of Naples Parthenope, 80143 Napoli, Italy
[3]Department of Electrical Engineering and Information, University of Cassino and Lazio Meridionale, 03043 Cassino, Italy
[4]Department of Electrical Engineering, Wrocław University of Science and Technology, 50-370 Wrocław, Poland

Corresponding author: Antonio Bracale (antonio.bracale@uniparthenope.it)

This work was supported by the University of Naples Parthenope in the framework of the project ''metodi per la pianificazione e gestione delle smart-grids'' under Grant DING 324.

ABSTRACT Waveforms distortion is a pressing concern in Smart Grids where a massive presence of new technologies in distributed energy resources and in advanced smart metering systems is expected. In this context, the increasing diffusion of high switching frequencies static converters and the growing usage of Power Line Communication push for research dealing with the assessment of waveforms with spectral components up to 150 kHz. The analysis of such waveforms is a challenge for researchers due to the contemporaneous presence of a high number of spectral components in the range of low- (up to 2 kHz) and high- (up to 150 kHz) frequencies, with their opposite needs in term of time window length (and frequency resolution). The main idea of this paper is to improve the performances of existing methods by using a joint method of analysis based on a profitable strategy of divide and conquer; the method guarantees the best compromise between accuracy and computational efforts. A Discrete Wavelet Transform initially divides the original waveform to obtain two frequency bands: the wavelet suitability for conducting multi-resolution time-frequency analysis on waveforms in different frequency bands with different frequency resolution is effectively exploited. Then, the sliding-window modified ESPRIT method and the sliding-window Discrete Fourier Transform which uses a Nuttal window are used for the analysis of the low- and high-frequency bands, respectively; the positive characteristics of each method are exploited, minimizing the drawbacks and integrating their behavior so that the whole joint method allows an accurate estimation of each low- and high-frequency spectral component with the required acceptable computational efforts. The proposed method is tested on synthetic and measured waveforms in terms of accuracy and computational efforts. The analysis of the numerical application results clearly reveals that the proposed method improves the performances of existing methods of analysis in the examined cases.

INDEX TERMS Power quality, waveform distortions, harmonic and supraharmonic assessment.

LIST OF PRINCIPAL SYMBOLS AND ABBREVIATIONS

PRINCIPAL SYMBOLS

a_0, b_0	DWT parameters
$a_j(n)$, $d_j(n)$	approximated and detailed time trends of the progressively-halved-band DWT waveform
a'_s	cosines coefficients of Nuttal window
$\hat{f}_0$	estimated power system frequency
f_s	sampling frequency
f_{mdf}	DWT maximum detectable frequency
f_{bs}	DWT bands' separation frequency
ψ^*	complex conjugate of the mother wavelet
$r\,(n)$	white noise
$x\,(n)$	original waveform
$x_u\,(n)$	windowed waveform
$x_{low}(n)$	low-frequency DWT output
$x_{high}(n)$	high-frequency DWT output

The associate editor coordinating the review of this manuscript and approving it for publication was Flavia Grassi.

$A_k, \varphi_k, f_k, \alpha_k$	amplitude, initial phase, frequency and damping factor of the ESPRIT k^{th} complex exponential
M_i	number of ESPRIT exponentials
N_{max}	number of DWT decomposition levels
N_s	number of samples of waveform $x(n)$
S	number of cosines of Nuttal window
T_s	sampling period
W_N	DFT of Nuttal window
W_R	DFT of rectangular window
w_N	Nuttal window in the time domain

ABBREVIATIONS

ESPRIT/EM	estimation of signal parameters via rotational invariant method/ESPRIT method
DFT	discrete Fourier transform
DPT	desynchronized processing technique
DWT	discrete wavelet transform
DWT-MEM	hybrid discrete wavelet transform - modified esprit method
HF	high-frequency signal
IECM1	DFT-based method in IEC 61000-4-7
IECM2	DFT-based method in IEC 61000-4-30
LF	low-frequency signal
MEM-DF Nuttal	proposed multi-step procedure using DWT, SWMEM and SWDFT with Nuttal window
PCC	point of common coupling
PLC	power line communication
SWDFT	sliding-window discrete Fourier transform
SWMEM	sliding-window modified ESPRIT method
TFR	time-frequency representation

I. INTRODUCTION

A. MOTIVATION OF THE RESEARCH

Smart Grid (SG) is a paradigm not univocally defined over the world [1]. As an example, the European Union point of view declares that: ''*A smart grid is an electricity network that can intelligently integrate the actions of all users connected to it − generators, consumers and those that do both − in order to efficiently deliver sustainable, economic and secure electricity supplies*''. Whatever the definition is, SG paradigm practical application unavoidably involves a wide deployment of new electrical and communication technologies. These new technologies include distributed energy resources (such as wind, solar power plants and storage systems), electric vehicle chargers, modern lightings and advanced smart metering systems which utilize high frequencies for power line communication (PLC) transmission.

The presence of these devices involves arduous electromagnetic compatibility problems to the planning and operation engineers due to the need of guaranteeing a satisfactory coexistence between sources of disturbances and susceptible loads.

Among disturbances, waveform distortions were of particular interest and widely investigated in the relevant literature.

Nowadays, the current and voltage waveforms distortions can be characterized by spectral components above the traditional 2 kHz harmonic frequency limit, in a range-extended up to 150 kHz. In contrast with the ''low-frequency distortion'' that usually ranges up to 2 kHz, the spectral content between 2 and 150 kHz was initially indicated as ''high-frequency distortion'', but recently the term ''supraharmonic'' was introduced and it is being used more frequently [2]–[6]. In this paper, we use the term high-frequency distortion and supraharmonic distortion indifferently for this range.

The high-frequency spectral components can be caused by both generators (e.g. photovoltaic power plants with their PWM controlled static converters) and loads (e.g. fluorescent lamps powered by high-frequency ballast and LED lamps). They can cause different problems in the electrical power systems, such as potential interferences with the power-line communication, errors in revenue meters and control systems, the possible appearance of both series and parallel resonance phenomena and reduction of life of electronic devices and network components.

Immunity and compatibility levels referred to supraharmonics are reported in Standards IEC 61000-4-19 and IEC 61000-2-2, respectively [7]. Due to the manner of interaction between the transmission systems and the power grid, it is worth comparing the compatibility levels and the immunity test levels with permissible levels of intentional emission. Fig. 1 presents several curves defined in the standards for the frequency range 2 – 150 kHz related to: intentional emission (i.e., mains signaling and power-line communication denoted in the figure by the lines described using the letter ''S''), compatibility levels in an electrical network (denoted in the figure using letter ''C'') as well as immunity test of the communication systems (denoted in the figure by the line described using the letter ''I'').

The above problems in the electrical power systems devices and the need to comply with electromagnetic compatibility levels push towards an accurate assessment of the supraharmonic spectral components in terms of both amplitude and frequency versus time.

B. BACKGROUND AND RELATED WORKS

The accurate assessment of supraharmonics is not an easy objective to be achieved due to several problems such as the different time-varying behavior and the conflicting needs in term of time window length and frequency resolution for the contemporaneous presence of both low- and high-frequency spectral components in the waveforms under analysis. In fact, the high-frequency distortion is generally characterized by components at frequencies that can be both correlated (*synchronous*) and not correlated (*asynchronous*) to the power system frequency; conversely, the low-frequency distortion

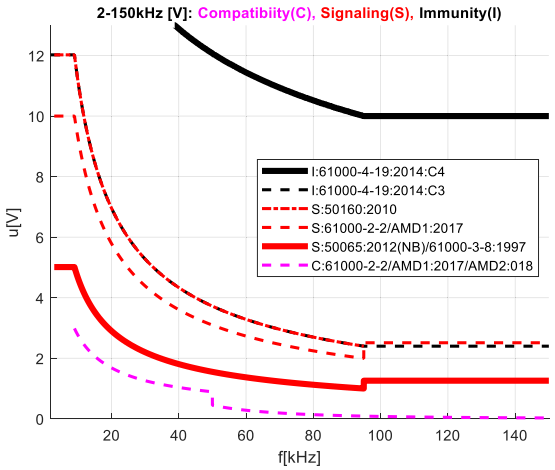

FIGURE 1. Mains signalling (S), compatibility (C) and immunity (I) levels for conducted disturbances in the frequency range 2-150 kHz.

is mainly constituted by only components at frequencies that are correlated to the power system frequency.

Both DFT-based and parametric techniques were proposed in the relevant literature for the spectral analysis of the above waveform distortions and, more generally, for their measurement. The first methods can suffer well known spectral leakage problems while the second methods can require high computational efforts while guaranteeing high results accuracy [8].

DFT-based methods in the supraharmonics measurement chain can be found in Standards IEC 61000-4-7 and IEC 61000-4-30 [9], [10]. Specifically, in the IEC Standard 61000-4-7 the grouping concept applied for the frequency range between 2 kHz and 9 kHz is extended up to 150 kHz even if the same Standard sees favourably research aiming at other techniques for the analysis of the high-frequency range. Comparisons between the above measurement methods are reported in [11]–[14]. The authors pointed at relevant limitations of DFT-based methods when the nonstationary character of the measured signals is considered. It was reflected that in the case of the signal components with variation in magnitude and/or in frequency the estimated magnitude values are usually underestimated due to the increasing leakage. To reduce the leakage effect and improve magnitude and frequency estimation, a suitable window length was discussed. Additionally, some remarks on the manner of performing the measurement intervals and analysis intervals were formulated. It was suggested to consider the application of the window synchronized with the fundamental frequency component as well as to keep the possible high-frequency resolution and avoid the gaps in time to preserve the reproducibility. Formulated requirements increase computational complexity.

Alternative measurement methods have been developed and compared using synthetic signals or recorded power system waveforms in [15]–[20]. In particular, in [15] a filter bank reduces the number of samples processed by the Fast Fourier Transform while the frequency resolution of supraharmonic is improved using the technique of compressive sensing. In [16] a high performing measurement algorithm is proposed based on multiple measurement vectors compressive sensing model and orthogonal matching pursuit recovery algorithm, which allows a supraharmonics analysis of an original spectrum array simultaneously through the least-squares method. In [17] a Bayesian compressive sensing is applied for further improving the supraharmonics frequency resolution. In [18] an advanced Wavelet-based hybrid method has been proposed for the simultaneous measurement of harmonic and supraharmonic distortion; the proposal seems to show robust characteristics against amplitude and power frequency deviations. In [19] a desynchronized processing technique (DPT) is applied as an effective alternative to the other digital filtering techniques presented in the literature. In [19], [20] also a comparison between currently existing measurement methods for 2 kHz to 150 kHz emissions in low voltage networks is reported. In particular, differences between methods are highlighted and their accuracy in identifying and measuring emissions is outlined. The conclusions are that the method based on wavelet decomposition can guarantee the same level of accuracy as the method for 2 kHz to 9 kHz in informative Annex B of IEC 61000-4-7 and desynchronized processing technique performs better than or as well as the other methods proposed in the literature in terms of magnitude response.

Finally, in [21] a two-step hybrid method (DWT-MEM) based on the successive use of a discrete wavelet transform (DWT) and a sliding-window modified ESPRIT method (SWMEM) was proposed. The DWT initially divides the original signal into low-frequency and high-frequency waveforms. Then, the SWMEM assesses spectral components of the two waveforms obtained as the output of the DWT-step. The method proposed in [21] was used in [22] to perform the grouping for both harmonic and supraharmonic distortions.

C. THE NEW PROPOSAL AND LIST OF KEY CONTRIBUTIONS

In this paper, a new joint method is proposed aiming to find the best compromise between spectral components accuracy and computational efforts in the assessment of actual power system waveforms including both harmonics and supraharmonics. The new proposal is based on a multi-step scheme where the DWT decomposition is applied at first to obtain two frequency (i.e., low- and high-frequency) bands; the low-frequency content (i.e., up to 2 kHz) is then analyzed by the SWMEM, whereas the high-frequency content (i.e., from 2 to 150 kHz) is analyzed by the SWDFT. A Nuttal sliding window [23] is applied to limit interference conditions between spectral components and better estimate synchronous and not synchronous supraharmonics.

The rationale of the proposal lies in the most useful use of both SWDFT which uses a Nuttal window and SWMEM with the constraint to maximize results accuracy and minimize computational efforts. In fact, we contend that SWMEM is an accurate and fast method especially when it analyzes waveforms with a reduced spectral content, which usually

requires a small sampling rate and a duration of the analysis windows multiple of the fundamental period. Conversely, the assessment of the high-frequency distortions, which usually require a large sampling rate and a small duration of the analysis window, is certainly faster by selecting SWDFT. On the other hand, due to the DWT decomposition and Nuttal window presence, the age-old leakage problems of SWDFT are expected to be minimized allowing an assessment of the high-frequency spectral components more accurate than those obtainable with SWDFT applied to the analysis of the whole original waveform.

To summarize, the key contributions of the paper are:

- a new joint method effectively integrating the positive characteristics of the discrete wavelet transform, the sliding-window modified ESPRIT method and the sliding-window DFT method is proposed;
- the discrete wavelet transform is applied exploiting its suitability for conducting multi-resolution time-frequency analysis on waveforms with different frequency resolution;
- the sliding-window modified ESPRIT is employed that focus on accurately estimating the low-frequency spectral components so allowing also an accurate value of the power system fundamental frequency;
- the sliding window DFT estimates the high-frequency spectral components with a Nuttal window synchronized to the fundamental frequency to mitigate spectral leakage and allow an accurate estimation of supraharmonics with reduced computational efforts;
- the joint method may provide accurate values of parameters (mainly, frequencies, amplitudes and initial phases) of low- and high-frequency spectral components meanwhile keep a relatively low computational cost;
- the joint method can be fully compliant with the IEC framework and can be used as a reference in laboratory measurements for research purposes for its accuracy; it is also more attractive for industrial applications since it significantly reduces the computational cost as compared with conventional parametric methods.

D. ORGANIZATION OF THE PAPER

The remainder of the paper is organized as follows. In Section II the proposed joint method is shown, including a brief theoretical presentation and a critical analysis of the SWMEM and SWDFT which uses a Nuttal window. Some related studies are reviewed to indicate recent results and formulate the crucial issues related to higher frequency spectrum analysis including time and frequency resolution, magnitude and frequency estimation errors as well as computational complexity. Section III presents numerical applications of the proposed method on synthetic and measured waveforms. The measured signal consists of higher frequency components related to photovoltaic and a power line communication system. Comparisons with the results obtained applying other methods proposed in the literature (ESPRIT method, DWT-MEM, DPT) and the IEC Standards methods are also provided. The comparisons are made in terms of the magnitude estimation including time variation as well as over and underestimation issues. The conclusions are in Section IV.

II. THE PROPOSED METHOD

In modern power systems, the current and voltage waveforms can be characterized by wide spectra including components that range up to 150 kHz.

Usually, this wide range is separated into two different bands including low-frequency (up to 2 kHz) and high-frequency (up to 150 kHz) spectral components, respectively; as it was previously evidenced, the high-frequency spectral components are also called supraharmonics.

The presence of the supraharmonics is caused by a lot of emitters such as converters for industrial applications, electronic device commutation, street lamps, electro-vehicle chargers, photovoltaic and wind turbine inverters, household devices, e.g., liquid-crystal display televisions or highly-efficient loads and PLC [24].

The superposition of low- and high-frequency spectral components pose challenges in the waveform distortion assessment due to the different and conflicting needs of the two bands.

The low-frequency spectral components are mainly constituted by spectral components at frequencies linked to the power system frequency. They include the well know harmonics, i.e. spectral components at frequencies that are integer multiples of the ac system fundamental frequency, and interharmonics, i.e., spectral components at frequencies that are not integer multiples of the system fundamental frequency.

Conversely, the high-frequency spectrum is generally characterized by spectral components at frequencies both correlated (*synchronous*) and not directly linked (*asynchronous*) to the ac system fundamental frequency. Moreover, they have fast dynamics, with frequencies and amplitudes that can rapidly vary vs. time, and an energy content usually very small if compared with the energy of harmonics [4], [5], [21], [24], [25].

The above mentioned substantially different and, in some cases, opposite characteristics make the waveform distortion assessment of a waveform including both low- and high-frequency spectral components a very challenging task that surely involves a point of view different from the traditional one adopted for the low-frequency components only.

In this paper, we propose to assess the waveform distortions of a wide spectrum including both low- and high-frequency components using a joint method that involves profitably three different methods of analysis.

A Discrete Wavelet Transform initially divides the original waveform to obtain two frequency (i.e., low- and high-frequency) bands exploiting the wavelet suitability for conducting multi-resolution time-frequency analysis on waveforms in different frequency bands with different frequency resolution. Then, the modified ESPRIT method is

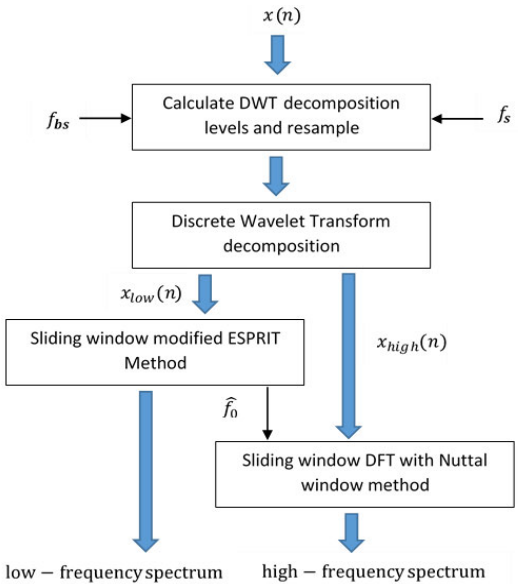

FIGURE 2. Scheme of the proposed method.

used for the analysis of the low-frequency band; the application of the ESPRIT method allows a very accurate calculation of the low-frequency spectral components, including the ac system fundamental parameters, with reduced computational efforts due to the low number of components involved. Finally, the sliding-window Discrete Fourier Transform which uses a Nuttal window is applied; a Nuttal window length multiple of the ac fundamental frequency, accurately furnished by the previous ESPRIT method application, guarantees a significant reduction of the spectral leakage in the calculation of synchronous and asynchronous supraharmonics, as well as the use of DFT, provides well know reduced computational efforts.

Summarizing, the proposed method is based on the following multi-step procedure (Fig. 2):

1st step: Calculate the number of the DWT decomposition level and resample the waveform under analysis;

2nd step: Apply DWT and select as output the low- and high-frequency signals;

3rd step: Apply SWMEM to the low-frequency signal and send the estimated fundamental frequency $\hat{f}_0$ to SWDFT block;

4rth step: Apply SWDFT which uses a Nuttal window of length synchronized with the estimated fundamental period to the high-frequency signal.

In the following subsections, the main features of each of these steps are described in detail.

A. FIRST STEP

In the first step, the number of the DWT decomposition level and the resample of the waveform under analysis are performed.

With reference to the DWT decomposition level, it should be noted that the DWT (see step 2) is often used as a filter bank, since it appears a sort of high and low pass band filters in cascade, with two bands of frequency obtained at each level. However, the bands are affected by overlap and attenuation at their edges. In the proposed method, multi-level DWT decomposition is achieved by assuming the following number N_{max} of decomposition levels [21], [26]:

$$N_{max} = \left\lceil \log_2 \left(\frac{f_{mdf}}{f_{bs}} \right) \right\rceil \tag{1}$$

where f_{mdf} is the maximum detectable frequency given by:

$$f_{mdf} = f_s/2 \tag{2}$$

being f_s the sampling frequency and f_{bs} the bands' separation frequency, i.e., the frequency that separates low- and high-frequency spectra; in this paper, following the IEC framework [9], [10], f_{bs} is fixed at 2 kHz.

Concerning the resample of the waveform under analysis, we adapt the sampling frequency to optimize the DWT use, avoiding filter bounds to be too close to the frequencies that must be detected.

B. SECOND STEP

In the second step, the DWT is applied and the low- and high-frequency signals are obtained as output. In this step, we exploit the wavelet suitability for conducting multi-resolution time-frequency analysis on waveforms in different frequency bands with different frequency resolution [26], [27]. Moreover, the DWT guarantees a waveform decomposition without phase shifting and leakage among bands.

As well known, the N_s-point DWT of a sequence of N_s samples of the sampled waveform $x(n)$ is given by:

$$DWT(j,k) = \frac{1}{\sqrt{a_0^j}} \sum_{n=0}^{N_s-1} x(n)\, \psi^* \left(\frac{n - k b_0 a_0^j}{a_0^j} \right) \tag{3}$$

where ψ^* is the complex conjugate of the mother wavelet to be chosen, j and k are integers and a_0 and b_0 are parameters to be chosen.

With reference to the mother wavelet, its choice is a crucial point. A wide number of mother wavelet has been applied, also in the field of power system waveform distortion assessment. In this paper, a Meyer mother wavelet is applied.

Concerning a_0 and b_0 parameters, their values help to dilate and translate the mother wavelet. In this paper, the scale parameter is discretized to integer powers and the translation parameter is proportional to the scale [28]. Once chosen mother wavelet and its parameters a_0 and b_0, the decomposition of the waveform under study is performed on the assigned N_{max} decomposition levels (Fig.3).

For each level, the waveform is split into two parts made up of high- and low-frequencies, with the low-frequencies passed at the next level and split again. The procedure is repeated N_{max} times. At each level j of decomposition, the DWT provides both the approximated a_j(n) and the

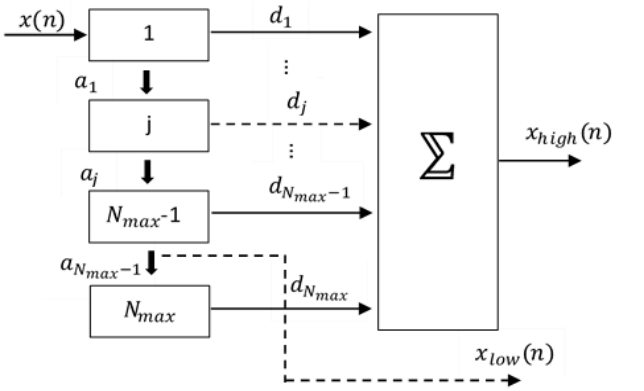

FIGURE 3. DWT decomposition scheme.

detailed $\boldsymbol{d_j(n)}$ time trends of the progressively-halved-band waveform.

Finally, the outputs of the DWT application are the waveforms $\boldsymbol{x_{low}}\,(\boldsymbol{n}) = \boldsymbol{a_{N_{max}-1}(n)}$ and $\boldsymbol{x_{high}}\,(\boldsymbol{n}) = \sum_{j=1}^{N_{max}} \boldsymbol{d_j(n)}$.

C. THIRD STEP

In this step, the sliding window modified ESPRIT method (SWMEM) is applied to the low-frequency signal $\boldsymbol{x_{low}}\,(\boldsymbol{n})$.

We remind that ESPRIT original method is a parametric method that expresses a waveform $x_u(n)$ of generic size L_i as a sum of exponentials, according to the following relationship [21]:

$$\hat{x}_u\,(n) = \sum_{k=1}^{M_i} A_k e^{j\varphi_k} e^{(\alpha_k + j2\pi f_k)nT_s} + r\,(n) \qquad (4)$$

with $n = 0, 1, \ldots, L_i - 1$, and where T_s is the sampling period and A_k, φ_k, f_k, and α_k are the unknown amplitude, initial phase, frequency and damping factor of the k^{th} complex exponential, respectively. The parameters and the number of exponential M_i are related to each window i of the segmented waveform and they have to be estimated by using the transformation properties of the rotation matrix associated with the waveform samples. In (4) $r\,(n)$ is the white noise.

The ESPRIT original method, and its sliding window version SWEM, have proved to be very accurate methods for the assessment of power system waveforms but their computational time was revealed very high since the need to solve cumbersome equations for each window inside the whole signal to be analyzed.

The sliding window modified ESPRIT method (SWMEM) applied in this paper modifies the sliding window ESPRIT's original approach in several important aspects and significantly reduces the computational efforts while saving result accuracy. The improvements are: (i) evaluating the frequencies and damping factors of exponentials one time or, at most, only a few times; (ii) evaluating the amplitudes and initial phases of the exponentials in all the time windows but with a significantly reduced computational effort.

This is obtained by the classification of the analysis windows in "basis windows" and "no-basis windows". In the basis windows, all the parameters (i.e., amplitude, initial phase, frequency and damping factor) of the ESPRIT original model are calculated for all of the spectral components included in the analyzed waveform $x_{low}\,(n) = \hat{x}_u\,(n)$ given by (4). The number of basis windows depends on a check on the reconstruction error, which has to be lower than a selected threshold. Conversely, in the no-basis window, only the amplitudes and the initial phases of the aforesaid model (4) are calculated for each spectral components since the frequencies and damping factors are considered piecewise constant and fixed equal to the values obtained in the last basis window.

It should be noted that thanks to the DWT decomposition in the second step, $x_{low}\,(n)$ includes a number of spectral components significantly lower than the original sequence $x\,(n)$ with obvious advantages in term of computational efforts. In addition, $x_{low}\,(n)$ can be downsampled to only two times the bands' separation frequency, reducing the number of samples in each window and, once again, the global computational efforts. It should be also noted that the application of the ESPRIT method to the low-frequency signal $x_{low}\,(n)$ allows a very accurate calculation of the ac system fundamental frequency with great advantages also in the calculation of the synchronous supraharmonics, as it will be detailed in the next subsection D.

For more details about SWMEM see [21].

D. FOURTH STEP

In this step, the sliding window DFT method (SWDFT) which uses a Nuttal window is applied to the high-frequency signal $\boldsymbol{x_{high}}\,(\boldsymbol{n})$.

As well known, the DFT is the most frequently applied method for the assessment of waveform distortions and it is universally adopted by Standards and Recommendations.

If a waveform $x_u(n)$ of generic size L_i is taken into account, its L_i-point DFT is given by:

$$DFT(k) = \sum_{n=0}^{L_i-1} x_u(n) e^{-j2\pi \frac{k}{L_i} n} \qquad (5)$$

with $k = 0, 1, \ldots, L_i - 1$.

The main problem with SWDFT technique leads to spectrum contamination by leakage. Several advanced approaches have been proposed to minimize spectral leakage problems in DFT application [8]. In this paper, the Nuttal window shown in the next subsection E is applied [23].

It should be noted that the knowledge of the ac system fundamental frequency obtained in step C and the use of Nuttal window offer several advantages in the calculation of supraharmonics, both synchronous and asynchronous. In fact, the application of:

(i) a Nuttal window length multiple of the ac fundamental frequency guarantees a reduction of the spectral leakage in the calculation of synchronous supraharmonics, for obvious reasons;

(ii) the Nuttal window guarantees a reduction of the spectral leakage in the calculation of asynchronous supraharmonics, for the reasons shown in the next subsection.

Eventually, note that thanks to the reduced spectral leakage in the high-frequency spectrum, shorter sliding time windows can be used to analyse $x_{high}(n)$ allowing the increase of accuracy of the proposed approach in case of time-varying supraharmonics.

E. NUTTAL WINDOW

As known, accurate results of DFT analysis are usually obtained using a rectangular window. However, in most practical cases the unknown value of the signal period to be analyzed and the presence of interharmonics can determine spectral leakage and picket fence effect phenomena. In the relevant literature, interpolation algorithms and alternative sliding windows have been proposed to improve the accuracy reducing the spectral leakage and picket fence effects [19], [29]–[39].

The Nuttall window is a generalized cosine window with favorable sidelobe characteristics that allow to significantly reduce the spectral leakage and picket fence effect. In fact, in desynchronized conditions: i) a large and flat central lobe reduces the amplitude attenuation of spectral components and ii) the interaction between adjacent tones depends on the amplitude of side lobes, thus the high attenuation of the Nuttal side lobes leads to a reduced or negligible interference between adjacent tones.

As a consequence, the ability of the window to reduce leakage is optimal. However, compared to the rectangular window, the main lobe width of Nuttall window is larger so that post-processing is needed to compensate the introduced systematic error; moreover, the possibility of detecting sinusoidal components close in frequency is not optimal (the frequency resolution is lower).

Fortunately, the frequency resolution problems in the Nuttal window use are not a matter in the analysis of supraharmonics since the high-frequency waveform spectral components in power systems are usually far in the frequency domain. Then, the Nuttall window application seems to be a good compromise for an accurate analysis of high-frequency waveform distortions in power systems.

In this paper, the symmetric Nuttall defined four-term window is used. The analytical expression of Nuttal window of generic size L_i in the discrete-time domain is [23], [40], [41]:

$$w_N(n) = \sum_{s=0}^{S-1} (-1)^s a'_s \cos\left(\frac{2\pi n}{N-1} s\right) \tag{6}$$

with $n = 0, 1, \ldots, L_i - 1$ and where $S = 3$ is the number of cosines of the window function, $a'_0 = 0.3635819$, $a'_1 = 0.4891775$, $a'_2 = 0.1365995$ and $a'_3 = 0.0106411$ that satisfy the following constraint: $\sum_{s=0}^{S-1} a'_s = 1$

In the frequency domain, the Nuttall window can be expressed as follows:

$$W_N(k) = \sum_{s=0}^{S-1} (-1)^s \frac{a'_s}{2} \left[W_R\left(k - \frac{2\pi}{L_i} s\right) + W_R\left(k + \frac{2\pi}{L_i} s\right) \right] \tag{7}$$

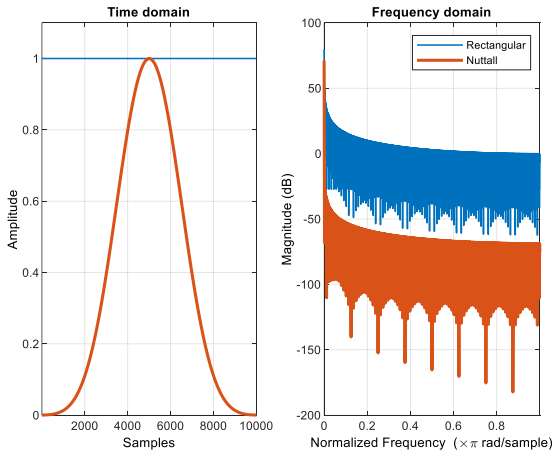

FIGURE 4. Time and frequency characteristics of Nutall window rectangular window representing 200 ms length with 50 kHz sampling.

with $k = 0, 1, \ldots, L_i - 1$ and where $W_R()$ is the discrete Fourier transform of a rectangular window.

The characteristics of four-term Nuttall DFT W_N are that: the central lobe includes seven spectral components, the maximum sidelobe is characterized by -96 dB, and the sidelobe decaying rate is 6 dB/octave. The central lobe is larger than the one of the rectangular window and a synchronized analysis of a single tone produces seven tones while only one tone derives from the use of the rectangular window. To account for this systematic error, all seven components are combined in a single spectral component at the central frequency applying a compensation gain calculated by equation (7).

An example of time and frequency characteristics of the Nuttall window and the rectangular window is presented in Fig. 4.

III. NUMERICAL APPLICATIONS

Numerical applications are related to the analysis of synthetic and measured waveforms. The synthesized waveforms include harmonics, interharmonics and supraharmonics due to different operating conditions of typical generation systems and loads in microgrids. For the sake of conciseness, only two case studies are reported in the following subsections. The first case study is related to the analysis of a synthetic waveform while the second case study refers to measured waveforms at the point of common coupling (PCC) of an actual PV system.

The proposed method, named in the following "MEM-DF Nuttal", is compared in terms of both computational burden and accuracy with: (i) the sliding window Esprit Method (EM) [42], i.e., a pure parametric method; (ii) the desynchronized processing technique (DPT) i.e., a DFT based method [19]; (iii) the sliding window Discrete Wavelet Transform Modified Esprit Method (DWT-MEM), proposed in [21]; and (iv) the DFT-based methods suggested in IEC 61000-4-7 (IECM1) and IEC 61000-4-30 (IECM2) for the analysis of waveforms with high-frequency spectral components [9], [10] (briefly recalled in Appendix for the sake of

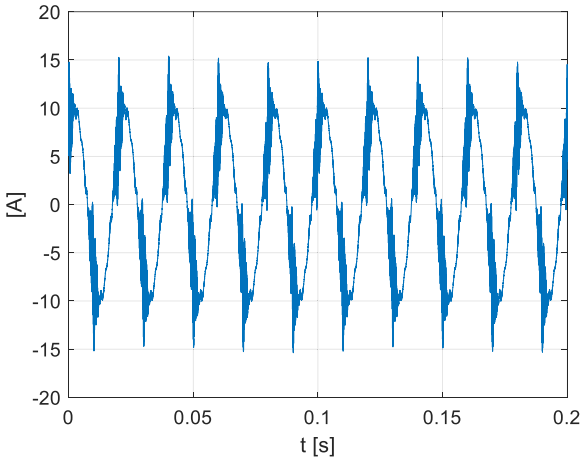

FIGURE 5. Case study 1: synthetic waveform.

clarity). DPT method was selected since it performs better than or as well as the other methods proposed in the literature in terms of magnitude response [19].

All analyses were performed using Matlab® programs developed and tested on a Windows PC with an Intel i7-3770 3.4 GHz and 16 GB of RAM.

A. SYNTHETIC WAVEFORM

The synthetic waveform is an acid test including harmonics, interharmonics and supraharmonics. They are typical spectral components that can be due to the background distortion and to the dispersed generation systems equipped with inverters utilizing high switching frequencies. The waveform under analysis is assumed to be a current characterized by a fundamental of 10 A at 50.02 Hz with all odd harmonics up to the 27th order (low-frequency harmonics), whose amplitudes are in the range [1.4-6] % of the fundamental component. The high-frequency content includes six spectral components due to the PWM technique of an inverter with a frequency modulation index m_f equal to 200 (the six components around the order $2m_f$-th); their amplitudes are fixed up to 2 % of the fundamental to emulate the behavior of the PV system during high-irradiance conditions [43]. Eventually, two desynchronized interharmonic tones at frequencies of 17598 Hz and 21997.5 Hz with amplitudes of 0.5 % of fundamental and white noise with a standard deviation of 0.001 are added.

The signal is 3 s long and its sampling frequency is 50 kHz (the first 200 ms are reported in Fig. 5). A resampling to 100 kHz is applied in the first step of the proposed method and the separation frequency f_{bs} is 2 kHz with $N_{max} = 5$. It results in a DWT sub-band tree in which the approximation on the level $N_{max} - 1$. For parametric methods, the error threshold was fixed to 10^{-5}.

Table 1 shows the average percentage errors of the frequencies (Tab. 1 a) and of the amplitudes (Tab. 1 b) for some spectral components obtained by the considered methods.

As expected, EM provided the most accurate estimation for all the spectral components, but this method required about 559 s to be applied. DPT partially reduce DFT problems; in fact, the results show that the it performs better than IEC methods mainly in terms of magnitude response.

Hybrid method DWT-MEM gave a solution of compromise between accuracy and computational efforts; in fact, the amplitudes and frequency errors were ever less than 0.17 % and the computational time was 6 s. The proposed method performs better than DPT and IEM methods providing errors similar to DWT-MEM, especially for supraharmonics synchronized with the actual fundamental frequency with a good behavior in amplitude assessment. The application of MEM-DF Nuttal required 0.8 s, thus it allowed a further reduction of computational time of about one order of magnitude with respect to DWT-MEM while it is slower than DPT that provided results in 0.05s. Note that the computational time is shorter than the sliding window duration (about one third).

IEC methods errors are the greatest for all spectral components since they were affected by spectral leakage problems due to the desynchronization of windows of analysis that increase as the frequency increases.

As expected, IECM1 and IECM2 provided similar results for low-frequency spectral components (lower than 2 kHz). In the high-frequency range (up to 150 kHz) the 200 Hz grouping aggregation of IECM1 reduced the amplitude errors of interharmonics (isolated spectral components) but increased the errors of adjacent synchronized supraharmonics due to PWM modulation since they are closer than 200Hz.

Concerning IECM2, the 2kHz grouping led to unacceptable amplitude errors for both synchronized and desynchronized supraharmonics due to the very low-frequency resolution.

The frequency errors of both IEC methods in the high-frequency range were similar and due to the reduced frequency resolution. Note also that the values are contained due to the high values of frequencies that reduce the percentage values.

Eventually, IEC methods were faster since they terminated the analysis in 0.02 s (IECM1) and 0.2 s (IECM2) with IECM2 slower due to the high number of sliding windows to analyze.

To better evidence the advantages of the proposed approach, Fig. 6 shows the main spectral components obtained using the proposed method and IECM1. For the sake of conciseness and clarity, the other spectra are omitted. Anyway, EM and DWT-MEM had results very similar to MEM-DF Nuttal while IECM2 had a behavior similar to IECM1. DPT is applied by using the Hanning window and the interpolation technique provided a behavior similar to MEM-DF Nuttal.

Fig. 6 a reports low-frequency spectra while in Fig. 6 b the high-frequency spectra are shown.

As expected, in Fig. 6 an IECM1 spectrum presents several spectral components due to spectral leakage caused by fundamental desynchronization. As known, these spurious

TABLE 1. Case study 1: (a) Mean frequency errors and (b) Mean amplitude errors in percentage.

(A)

Freq. [Hz]	EM	DPT	DWT-MEM	IEC M1	IEC M2	MEM-DF Nuttal
50.02	8.44×10^{-12}	0.040	1.02×10^{-4}	0.04	0.04	3.98×10^{-5}
3rd	1.96×10^{-11}	0.040	5.42×10^{-5}	0.04	0.04	6.69×10^{-4}
11th	6.77×10^{-12}	0.040	2.78×10^{-5}	0.04	0.04	1.41×10^{-4}
13th	1.48×10^{-12}	0.040	2.57×10^{-4}	0.04	0.04	3.68×10^{-5}
395th	1.38×10^{-13}	0.040	5.24×10^{-5}	0.29	1.22	1.60×10^{-5}
397th	9.83×10^{-14}	0.040	3.24×10^{-5}	0.21	0.71	1.60×10^{-5}
399th	9.17×10^{-14}	0.040	5.29×10^{-5}	0.29	0.21	1.60×10^{-5}
401th	6.80×10^{-14}	0.040	7.16×10^{-5}	0.21	0.29	1.60×10^{-5}
403th	9.09×10^{-14}	0.040	6.25×10^{-5}	0.29	0.78	1.60×10^{-5}
405th	1.31×10^{-13}	0.040	7.14×10^{-5}	0.21	1.27	1.60×10^{-5}
17598	9.50×10^{-13}	0.034	1.51×10^{-5}	0.56	2.28	5.54×10^{-3}
21997.5	8.60×10^{-13}	0.027	7.50×10^{-5}	0.44	0.01	5.69×10^{-3}

(B)

Freq. [Hz]	EM	DPT	DWT-MEM	IEC M1	IEC M2	MEM-DF Nuttal
50.02	7.11×10^{-10}	3.17×10^{-5}	7.05×10^{-4}	0.01	0.01	5.50×10^{-4}
3rd	3.19×10^{-8}	3.11×10^{-4}	1.52×10^{-2}	0.61	0.62	1.57×10^{-2}
11th	9.34×10^{-9}	3.91×10^{-3}	4.10×10^{-3}	0.23	0.23	5.05×10^{-3}
13th	2.08×10^{-8}	5.57×10^{-3}	1.01×10^{-2}	0.58	0.58	2.97×10^{-3}
395th	2.05×10^{-8}	10.8×10^{-1}	3.74×10^{-2}	13.4	355	2.14×10^{-4}
397th	6.89×10^{-9}	10.4×10^{-1}	1.15×10^{-2}	63.6	51.9	2.09×10^{-3}
399th	5.53×10^{-9}	10.9×10^{-1}	3.20×10^{-2}	22.7	13.9	2.89×10^{-4}
401th	5.55×10^{-9}	9.71×10^{-1}	2.20×10^{-2}	23.9	13.9	1.40×10^{-3}
403th	6.67×10^{-9}	9.34×10^{-1}	9.50×10^{-3}	65.6	51.9	1.90×10^{-3}
405th	1.93×10^{-8}	8.98×10^{-1}	4.32×10^{-2}	22.2	355	5.50×10^{-3}
17598	1.18×10^{-7}	8.743	17.7×10^{-2}	24.6	85.7	4.51×10^{-1}
21997.5	1.11×10^{-7}	10.111	5.59×10^{-2}	21.8	123	21.9×10^{-1}

spectral components determine a reduction of the amplitude of actual harmonics and interferences between them, leading to the errors reported in Table 1 b. The proposed method (bins in red) provided a clear spectrum and does not suffer spectral leakage problems since it uses EM for the analysis.

With reference to supraharmonics (Fig. 6 b), the results evidenced that IECM1 provided several spurious spectral components far from the actual values of both PWM synchronized tones and the two desynchronized interharmonics. The presence of several spurious spectral components and the significant amplitude errors were due to DFT spectral leakage and the IECM1 grouping aggregation of more components (closer than 200 Hz) in successive adjacent 200 Hz bands starting from 2 kHz.

The wrong allocation in the frequency of IECM1 bins was due to the fixed time window length of 200 ms, not linked to the actual value of the fundamental period. Instead (Fig. 6 b) MEM-DF Nuttal accurately allocated the red bins thanks to an accurate evaluation of the fundamental period by EM.

Eventually, the two interharmonics were visible only in MEM-DF Nuttal spectrum (Fig. 6b) with a minor spectral leakage for the 21997.5 Hz tone.

B. MEASURED WAVEFORMS

The waveforms under analysis were measured at PCC of the photovoltaic system reported in Fig. 7 that is based on three independent PV generation subsystems interfaced with the LV network by three 5 kVA dedicated single-phase inverters. The PV subsystems use different types of PV technologies on the three phases: phase L1 - monocrystalline; phase L2 - thin layer copper indium gallium selenide; and phase L3 - polycrystalline. Phases L1 and L3 have transformerless inverters.

At PCC a broad-band power line communication system is installed with Differential Code Shift Keying modulation in ''CENELEC A'' band (3-95 kHz) [44]. The technology is provide by Yitran Communications (US patent No. 6,064,695). The communication data are transmitted simultaneously in three bands that partially overlap: 18-44 kHz, 38-63 kHz and 58-89 kHz. In order to identify the magnitudes of the PLC transmission signal a data acquisition system based on a 16 bits DAQ card characterized by a sampling rate of 1.25 MHz was used.

Switching frequency of single-phase inverters is 16 kHz. Thus PWM modulation tones at frequencies integer multiple of the switching frequency (i.e., 16 kHz, 32 kHz, 48 kHz, 64 kHz, 80 kHz) are expected in the spectrum of voltages.

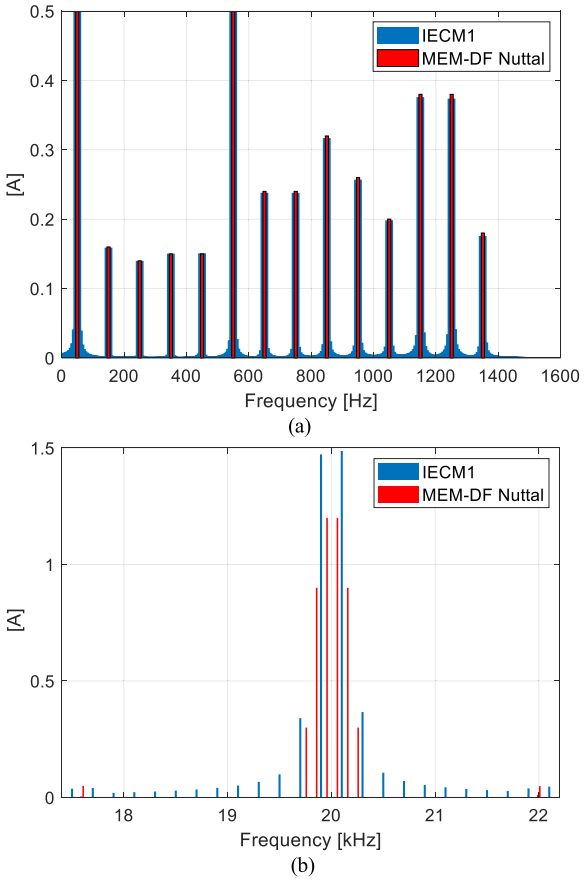

FIGURE 6. Synthetic waveform: spectra at low (a) and high (b) frequencies using IECM1 and MEM-DF Nuttal.

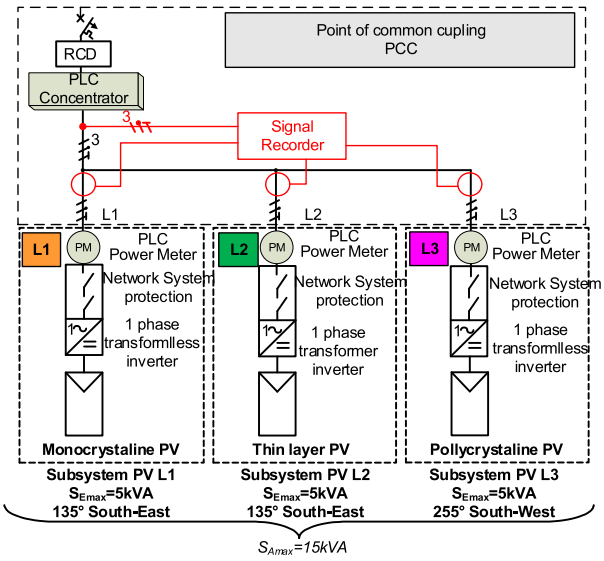

FIGURE 7. Scheme of PV system of measured waveforms.

The amplitudes are depending on irradiation conditions. Note that the subsystem associated with phase L3 is localized in different geographical direction (255° South-West), thus irradiation and, then, generation of phase L3 has a natural delay

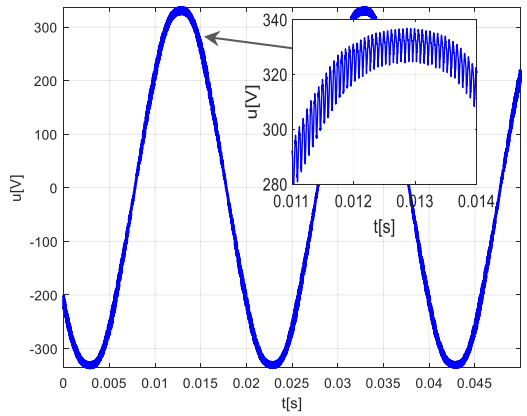

FIGURE 8. Measured voltage on phase L1.

in energy production. Eventually, on phase L3 the spectral components due to PLC communication data are expected from 2 s to 4 s.

In the following, the results of the spectral analysis on the phase voltages at PCC were reported and discussed. For the sake of conciseness, only the results of EM, DPT, MEM-DF Nuttal and IECM1 were shown. Anyway, DWT-MEM had results very similar to EM and MEM-DF Nuttal while IECM2 had a behavior similar to IECM1. EM results will be considered as the reference for their known high level of accuracy [21].

As an example, Fig. 8 shows the measured voltage on phase L1 with also the high-frequency spectral content evidenced.

Figs. 9 report the time-frequency representation (TFR) of the voltages on phase L1 (Fig. 9a), L2 (Fig. 9b) and L3 (Fig. 9c) in the range of supraharmonics from 10 kHz to 50 kHz obtained applying the proposed method MEM-DF Nuttal. In Figs. 10 the TFRs concerning the range from 50 kHz to 100 kHz are shown.

The Figs. 9 and 10 analysis shows that the main components were around integer multiple of the switching frequency of the PV inverters (i.e., 16 kHz, 32 kHz, 48 kHz, 64 kHz, 80 kHz). However, TFR on phase L1 contains the most significant contribution with values of amplitude that reach 2% of the fundamental. This is due to a significant production of PV energy on phase L1. In Fig. 9c and Fig. 10c spectral components due to the PLC transmission in the range from 20 to 40 kHz (Fig. 9c) and from 50 to 80 kHz (Fig. 10c) were observable from 2 s to 4 s. The challenge for the spectrum estimation methods is that the magnitude of the PLC transmission signals is relatively small and are affected by PWM inverter modulation tones.

To compare the results with EM, DPT and IECM1, the amplitudes versus time of the main supraharmonics were reported in Figs 11. In particular, Fig. 11a shows the main component (close to 16 kHz) due to PWM modulation related to voltage on phase L1 obtained applying the considered methods while in Fig. 11b, the spectral component due to PLC with the greatest amplitude is reported.

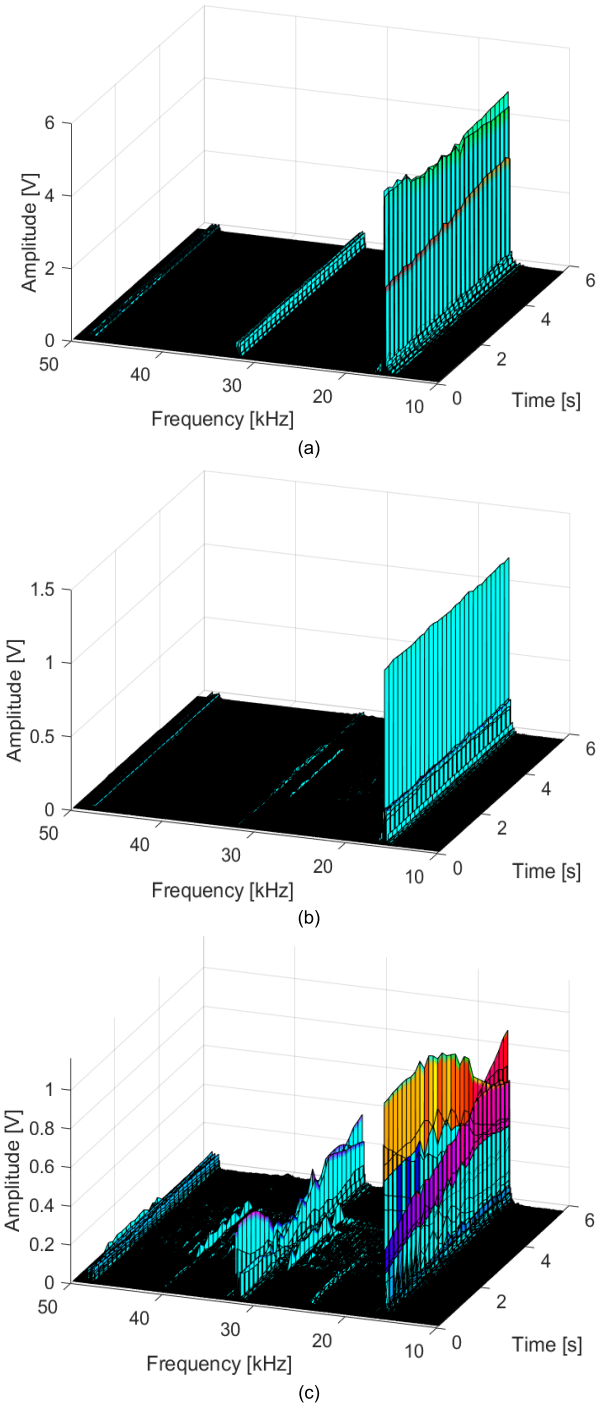

FIGURE 9. TFR in [10 50] kHz of measured voltage obtained by MEM-DF Nuttal: phase L1 (a), phase L2 (b) and phase L3 (c).

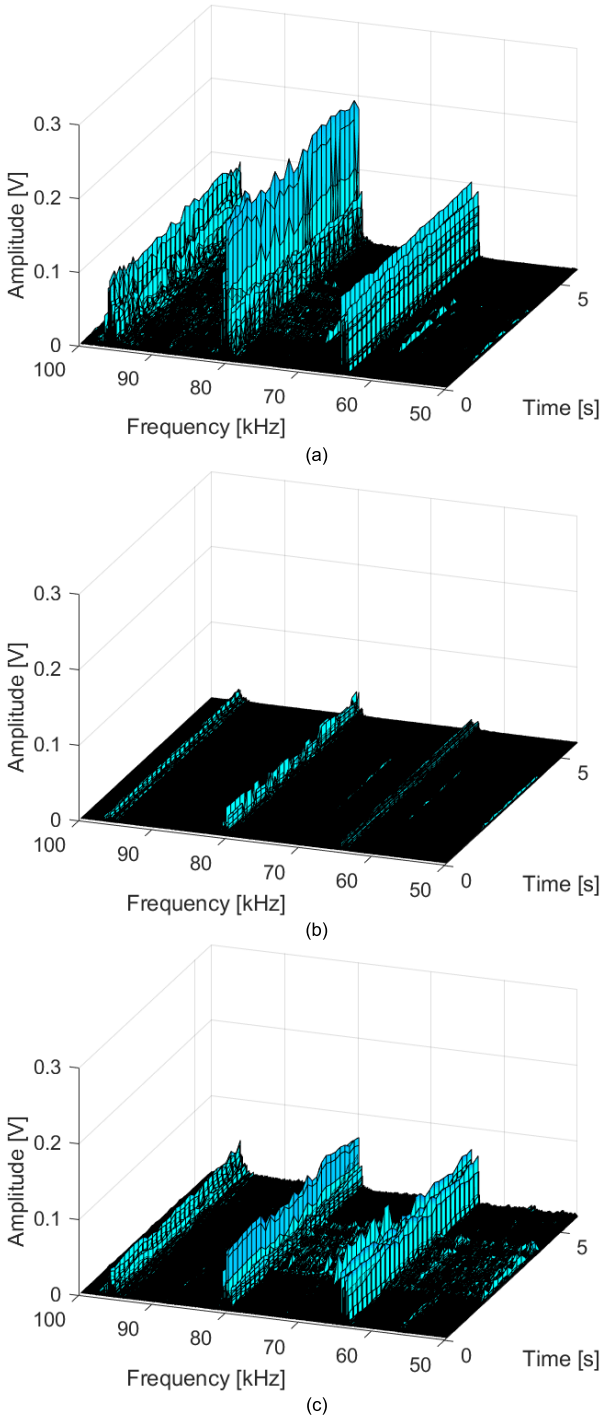

FIGURE 10. TFR in [50 100] kHz of measured voltage obtained by MEM-DF Nuttal: phase L1 (a), phase L2 (b) and phase L3 (c).

From Figs. 11 it appears that:

- EM was characterized by more rapid time variation linked to the shorter sliding time windows used for the analysis;
- thanks to the interpolation technique, DPT provided a behavior similar to MEM-DF Nuttal for supraharmonics, with a reduction of spectral leakage phenomenon. However, with respect to EM, an underestimation of PWM tones amplitudes is observed;
- the proposed method provided results similar to average values of EM while IECM1 is characterized by an overestimation of PWM tones amplitudes due to the DFT leakage and the 200 Hz grouping;
- all methods estimated a PLC tone with significant amplitude between 2s and 4s (Fig.9b). Once again, the

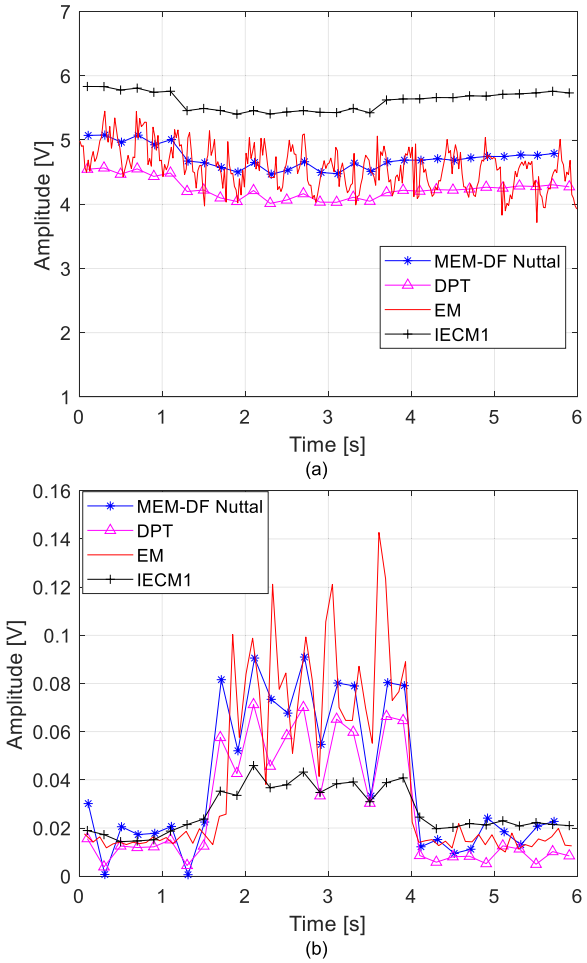

FIGURE 11. Supraharmonic amplitude estimation of PWM (a) and PLC (b) spectral component amplitudes applying MEM-DF Nuttal, DPT, EM, IECM1.

proposed method provided results similar to EM while IECM1 underestimated the amplitude of PLC component due to the spectral leakage;
- the proposed method provided results similar to average values of EM while DPT confirmed an underestimation of PLC tone.

IV. CONCLUSION

A joint method based on parametric sliding window Modified Esprit and traditional sliding window DFT method with the use of Nuttal window has been proposed for the spectral analysis of waveforms characterized by spectral components up to 150 kHz. The method starts from a DWT decomposition of the original signal into low-frequency and high-frequency waveforms.

The low-frequency waveform is analyzed with the modified sliding window Esprit method to obtain an accurate estimation of low-frequency spectral components and a precise estimation of the fundamental frequency. The high-frequency waveform is analyzed by using the DFT with a synchronized Nuttal sliding time window to obtain accurate and fast time-frequency representation of supraharmonics.

The proposed method was tested and evaluated on synthetic and measured waveforms on an actual PV system. Results have shown that the proposed joint method is effective and efficient in terms of accurately estimating spectral components up to 150 kHz as well as computational speed. An accurate estimation of time-varying spectral components is obtained at very high frequency resolution while the spectral leakage is mitigated from using synchronized analysis windows.

The main outcomes of the method are that it:

- Yielded an accurate estimation of all the spectral components up to 150 kHz.
- Resulted in highly accurate harmonic estimates due to the use of the sliding window ESPRIT. An accurate value of the fundamental frequency was also obtained.
- Significantly reduced the estimation error of supraharmonics by using a Nuttal analysis window synchronized to the accurate fundamental frequency.
- Resulted in a significant reduction of the computational time as compared with the conventional sliding window ESPRIT applied to the full band data sequence without sacrificing the performance of estimation that, anyway, performs better than or as well as other methods proposed in the literature for the case studies shown.
- Since the computational time is shorter than the sliding window duration, the proposed method can be more attractive in the framework of in situ power quality monitoring.

Future work includes more systematic tests of the proposed scheme using large numbers of recorded waveforms from measurements. Moreover, also waveforms including more supraharmonics sources will be analyzed.

APPENDIX

In this Section the methods IECM1 and IECM2 suggested in [9], [10] are briefly recalled.

The method IECM1 was introduced in Standard [9]. Concerning the low-frequency spectral content, it suggests the use of the traditional DFT with a rectangular window of 10 (12) times the fundamental period. For measurements in the frequency range 2-9 kHz, Annex B of the same Standard indicates the use of DFT with a sliding rectangular window of 200 ms independent of the fundamental period. The spectral components obtained by DFT are, then, grouped in successive adjacent 200 Hz bands starting from 2 kHz using the root sum square. In Annex C of [10], the method is extended for measurements in the frequency range 9-150 kHz.

The method IECM2 is introduced in Annex C of informative Standard [10] as an alternative to the method suggested in [9] for measurement of supraharmonics.

The method includes four successive steps:

i. resample the waveform with a sampling frequency of 1024 kHz and apply high pass filter for damping the low-frequency components below 9 kHz;

ii. use a sliding rectangular window of 10 (12) cycles for 50 (60) Hz networks to define the analysis intervals;
iii. for each analysis interval, apply DFT to 32 measurement intervals of 512 samples (0.5 ms) equally distributed over the interval (corresponding to 2kHz);
iv. spectral components obtained by DFT in step iii) are aggregated in time and minimum, maximum, and RMS values are calculated for each analysis interval.

Eventually, high pass Butterworth filters are used for both IEC methods and the parameters of the digital filters are reported in [45].

REFERENCES

[1] M. Shabanzadeh and M. P. Moghaddam, "What is the smart grid? Definitions, perspectives, and ultimate goals," in *Proc. 28th Power Syst. Conf.*, Tehran, Iran, Nov. 2013, pp. 1–5.

[2] J. Meyer, M. Bollen, H. Amaris, A. M. Blanco, A. G. de Castro, J. Desmet, M. Klatt, L. Kocewiak, S. Rönnberg, and K. Yang, "Future work on harmonics—Some expert opinions Part II—Supraharmonics, standards and measurements," in *Proc. 16th IEEE Int. Conf. Harmon. Qual. Power (ICHQP)*, Bucharest, Romania, May 2014, pp. 909–913.

[3] A. Emanuel and A. McEachern, "Electric power definitions: A debate," in *Proc. IEEE Power Energy Soc. Gen. Meeting*, Vancouver, BC, Canada, Jul. 2013, pp. 21–25.

[4] A. Moreno-Munoz, A. Gil-de-Castro, E. Romero-Cavadal, S. Ronnberg, and M. Bollen, "Supraharmonics (2 to 150 kHz) and multi-level converters," in *Proc. IEEE 5th Int. Conf. Power Eng., Energy Electr. Drives (POWERENG)*, Riga, Latvia, May 2015, pp. 37–41.

[5] H. Renner, B. Heimbach, and J. Desmet, "Power quality and electromagnetic compatibility: Special report session 2," in *Proc. 23rd Int. Conf. Exhib. Electr. CIRED*, Lyon, France, Jun. 2015, pp. 1–37.

[6] E. O. A. Larsson and M. H. J. Bollen, "Measurement result from 1 to 48 fluorescent lamps in the frequency range 2 to 150 kHz," in *Proc. 14th Int. Conf. Harmon. Qual. Power (ICHQP)*, Bergamo, Italy, Sep. 2010, pp. 1–8.

[7] A. Espín-Delgado, S. K. Rönnberg, and M. Bollen, "Uncertainties in the quantification of supraharmonic emission: Variations over time," in *Proc. 18th Int. Conf. Renew. Energies Power Qual. (ICREPQ)*, Granada, Spain, Apr. 2020, pp. 1–6.

[8] P. Caramia, G. Carpinelli, and P. Verde, *Power Quality Indices in Liberalized Markets*. London, U.K.: Wiley, 2009.

[9] *General Guide on Harmonics and Interharmonics Measurements, for Power Supply Systems and Equipment Connected Thereto*, IEC Standard 61000-4-7, International Electrotechnical Commission, Geneva, Switzerland, 2010.

[10] *Testing and Measurement Techniques-Power Quality Measurement Methods*, IEC Standard 61000-4-30, International Electrotechnical Commission, Geneva, Switzerland, 2015.

[11] M. Klatt, J. Meyer, and P. Schegner, "Comparison of measurement methods for the frequency range of 2 kHz to 150 kHz," in *Proc. 16th Int. Conf. Harmon. Qual. Power (ICHQP)*, Bucharest, Romania, May 2014, pp. 818–822.

[12] G. Anne, M. Jan, and R. Sarah, "Comparison of measurement methods for the frequency range 2–150 kHz (supraharmonics)," in *Proc. IEEE 9th Int. Workshop Appl. Meas. Power Syst. (AMPS)*, Bologna, Italy, Sep. 2018, pp. 1–6.

[13] T. M. Mendes, C. A. Duque, L. R. M. da Silva, D. D. Ferreira, J. Meyer, and P. F. Ribeiro, "Comparative analysis of the measurement methods for the supraharmonic range," *Int. J. Electr. Power Energy Syst.*, vol. 118, Jun. 2020, Art. no. 105801.

[14] V. Khokhlov, J. Meyer, A. Grevener, T. Busatto, and S. Ronnberg, "Comparison of measurement methods for the frequency range 2–150 kHz (supraharmonics) based on the present standards framework," *IEEE Access*, vol. 8, pp. 77618–77630, 2020.

[15] T. M. Mendes, C. A. Duque, L. R. M. Silva, D. D. Ferreira, and J. Meyer, "Supraharmonic analysis by filter bank and compressive sensing," *Electr. Power Syst. Res.*, vol. 169, pp. 105–114, Apr. 2019.

[16] S. Zhuang, W. Zhao, R. Wang, Q. Wang, and S. Huang, "New measurement algorithm for supraharmonics based on multiple measurement vectors model and orthogonal matching pursuit," *IEEE Trans. Instrum. Meas.*, vol. 68, no. 6, pp. 1671–1679, Jun. 2019.

[17] S. Zhuang, W. Zhao, Q. Wang, Z. Wang, L. Chen, and S. Huang, "A high-resolution algorithm for supraharmonic analysis based on multiple measurement vectors and Bayesian compressive sensing," *Energies*, vol. 12, no. 13, p. 2559, Jul. 2019.

[18] S. Lodetti, J. Bruna, J. J. Melero, V. Khokhlov, and J. Meyer, "A robust wavelet-based hybrid method for the simultaneous measurement of harmonic and supraharmonic distortion," *IEEE Trans. Instrum. Meas.*, vol. 69, no. 9, pp. 6704–6712, Sep. 2020.

[19] A. J. Collin, S. Z. Djokic, J. Drapela, R. Langella, and A. Testa, "Proposal of a desynchronized processing technique for assessing high-frequency distortion in power systems," *IEEE Trans. Instrum. Meas.*, vol. 68, no. 10, pp. 3883–3891, Oct. 2019.

[20] D. Ritzmann, S. Lodetti, D. de la Vega, V. Khokhlov, A. Gallarreta, P. Wright, J. Meyer, I. Fernández, and D. Klingbeil, "Comparison of measurement methods for 2–150-kHz conducted emissions in power networks," *IEEE Trans. Instrum. Meas.*, vol. 70, pp. 1–10, 2021.

[21] L. Alfieri, A. Bracale, G. Carpinelli, and A. Larsson, "A wavelet-modified ESPRIT hybrid method for assessment of spectral components from 0 to 150 kHz," *Energies*, vol. 10, no. 1, p. 97, Jan. 2017.

[22] L. Alfieri, A. Bracale, G. Carpinelli, and A. Larsson, "Accurate assessment of waveform distortions up to 150 kHz due to fluorescent lamps," in *Proc. 6th Int. Conf. Clean Electr. Power (ICCEP)*, Santa Margherita Ligure, Italy, Jun. 2017, pp. 636–644.

[23] A. Nuttall, "Some windows with very good sidelobe behavior," *IEEE Trans. Acoust., Speech, Signal Process.*, vol. ASSP-29, no. 1, pp. 84–91, Feb. 1981.

[24] L. Alfieri, A. Bracale, and A. Larsson, "New power quality indices for the assessment of waveform distortions from 0 to 150 kHz in power systems with renewable generation and modern non-linear loads," *Energies*, vol. 10, no. 10, p. 1633, Oct. 2017.

[25] M. Di Manno, P. Varilone, P. Verde, M. De Santis, C. Di Perna, and M. Salemme, "User friendly smart distributed measurement system for monitoring and assessing the electrical power quality," in *Proc. AEIT Int. Annu. Conf. (AEIT)*, Naples, Italy, Oct. 2015, pp. 1–5.

[26] J. Barros, R. I. Diego, and M. de Apraiz, "Applications of wavelet transform for analysis of harmonic distortion in power systems: A review," *IEEE Trans. Instrum. Meas.*, vol. 61, no. 10, pp. 2604–2611, Oct. 2012.

[27] P. F. Ribeiro, *Time-Varying Waveform Distortions in Power Systems*. Chippenham, U.K.: Wiley, 2009.

[28] I. Daubechies, *Ten Lectures on Wavelets*. Philadelphia, PA, USA: Society for Industrial and Applied Mathematics, 1992.

[29] J. Barros and R. I. Diego, "On the use of the hanning window for harmonic analysis in the standard framework," *IEEE Trans. Power Del.*, vol. 21, no. 1, pp. 538–539, Jan. 2006.

[30] D. Gallo, R. Langella, and A. Testa, "Desynchronized processing technique for harmonic and interharmonic analysis," *IEEE Trans. Power Del.*, vol. 19, no. 3, pp. 993–1001, Jul. 2004.

[31] A. Testa, D. Gallo, and R. Langella, "On the processing of harmonics and interharmonics: Using hanning window in standard framework," *IEEE Trans. Power Del.*, vol. 19, no. 1, pp. 28–34, Jan. 2004.

[32] T. Su, M. Yang, T. Jin, and R. C. C. Flesch, "Power harmonic and interharmonic detection method in renewable power based on nuttall double-window all-phase FFT algorithm," *IET Renew. Power Gener.*, vol. 12, no. 8, pp. 953–961, Jun. 2018.

[33] K. F. Chen and S. L. Mei, "Composite interpolated fast Fourier transform with the hanning window," *IEEE Trans. Instrum. Meas.*, vol. 59, no. 6, pp. 1571–1579, Jun. 2010.

[34] M. Mottaghi-Kashtiban and M. G. Shayesteh, "New efficient window function, replacement for the Hamming window," *IET Signal Process.*, vol. 5, no. 5, p. 499, 2011.

[35] H. Wen, J. Zhang, Z. Meng, S. Guo, F. Li, and Y. Yang, "Harmonic estimation using symmetrical interpolation FFT based on triangular self-convolution window," *IEEE Trans. Ind. Informat.*, vol. 11, no. 1, pp. 16–26, Feb. 2015.

[36] K. Duda, "DFT interpolation algorithm for Kaiser–Bessel and Dolph–Chebyshev windows," *IEEE Trans. Instrum. Meas.*, vol. 60, no. 3, pp. 784–790, Mar. 2011.

[37] B. Y. Qing, Z. S. Teng, Y. P. Gao, and H. Wen, "An approach for electrical harmonic analysis based on Nuttall window double-spectrum-line interpolation FFT," *Proc. CSEE*, vol. 28, no. 25, pp. 1–6, 2008.

[38] H. Wen, Z. Teng, Y. Wang, and X. Hu, "Spectral correction approach based on desirable sidelobe window for harmonic analysis of industrial power system," *IEEE Trans. Ind. Electron.*, vol. 60, no. 3, pp. 1001–1010, Mar. 2013.

[39] H. Wen, Z. Teng, Y. Wang, B. Zeng, and X. Hu, "Simple interpolated FFT algorithm based on minimize sidelobe windows for power-harmonic analysis," *IEEE Trans. Power Electron.*, vol. 26, no. 9, pp. 2570–2579, Sep. 2011.
[40] S. L. Marple, *Digital Spectral Analysis: With Applications*. Upper Saddle River, NJ, USA: Prentice-Hall, 1986.
[41] T. Jin, Y. Chen, and R. C. C. Flesch, "A novel power harmonic analysis method based on nuttall-kaiser combination window double spectrum interpolated FFT algorithm," *J. Electr. Eng.*, vol. 68, no. 6, pp. 435–443, Nov. 2017.
[42] A. Bracale, G. Carpinelli, I. Y.-H. Gu, and M. H. J. Bollen, "A new joint sliding-window ESPRIT and DFT scheme for waveform distortion assessment in power systems," *Electr. Power Syst. Res.*, vol. 88, pp. 112–120, Jul. 2012.
[43] D. Gallo, C. Landi, and M. Luiso, "AC and DC power quality of photovoltaic systems," in *Proc. IEEE Int. Instrum. Meas. Technol. Conf. (IMTC)*, Graz, Austria, May 2012, pp. 576–581.
[44] *Signalling on Low-Voltage Electrical Installations in the Frequency Range 3 kHz to 148,5 kHz—Part 1. General Requirements, Frequency Bands and Electromagnetic Disturbances*, EN Standard 50065-1:2012, 2012.
[45] A. J. Collin, R. Langella, A. Testa, S. Z. Djokic, and J. Drapela, "Assessing distortion within the IEC framework in the presence of high frequency components: Some considerations on signal processing," in *Proc. IEEE 9th Int. Workshop Appl. Meas. Power Syst. (AMPS)*, Bologna, Italy, Sep. 2018, pp. 1–6.

GUIDO CARPINELLI (Member, IEEE) received the M.Sc. degree in electrical engineering from the University of Naples Federico II, Italy, in 1978. He is currently retired and was a Professor of Electrical Energy Systems with the University of Naples Federico II. He has authored several articles in journals published by the IEEE, IEE, IET, and Elsevier. He has published a book on power quality indices edited by J. Wiley and has coauthored several book chapters. His research interests include power quality and power system analysis.

ANTONIO BRACALE (Senior Member, IEEE) received the degree in telecommunication engineering from the University of Napoli Federico II, Italy, in 2002, and the Ph.D. degree in electrical energy conversion from the Second University of Napoli, Italy, in 2005. He is currently an Associate Professor of Electrical Power System with the Department of Engineering, University of Napoli Parthenope, Italy. His research interests include power quality, power systems analysis, and energy forecasting.

PIETRO VARILONE (Member, IEEE) received the M.S. degree in electrical engineering from the University of Cassino, Italy, in 1995, and the Ph.D. degree in electrical energy conversion from the Second University of Napoli, Italy, in 1999. He is currently an Associate Professor of Power Systems with the Department of Electrical and Information Engineering "Maurizio Scarano," University of Cassino and Southern Lazio, Italy. His current research interests include the analysis of transmission and distribution unbalanced systems, and power quality issues, with particular attention to voltage sags, development of distribution networks toward smart grids.

TOMASZ SIKORSKI (Member, IEEE) received the Ph.D. degree in application of time–frequency analysis in electrical power systems from the Wrocław University of Science and Technology, Poland, in 2005, and the habilitation degree, in 2014. In 2006, he was a Postdoctoral Researcher with the Laboratory of Brian Science, RIKEN Institute, Tokyo. From 2006 to 2010, he led the postdoctoral project founded by the Polish Ministry of Higher Education and Science dedicated to application of novel signal processing methods in the analysis of power quality disturbances in powers systems with distributed generation. He became the University Professor, in 2016. He cooperates with industry and power system operators on monitoring, detection, and analysis of conducted disturbances and time-varying phenomena in power systems.

PAWEL KOSTYLA received the D.Sc. degree from the Wrocław University of Science and Technology, in 1998. Since 1999, he has been working as an Assistant Professor with the Department of Electrical Engineering. He holds the position of the Laboratory Manager of Theoretical Electrical Engineering. His research interests include artificial neural networks and methods of digital signal processing in automation and electrical engineering, algorithms of digital signal processing and electrical measurements, development and testing of new methods of measuring electrical parameters, and quality of electricity.

ZBIGNIEW LEONOWICZ (Senior Member, IEEE) received the M.S. and Ph.D. degrees in electrical engineering from the Wrocław University of Science and Technology, in 1997 and 2001, respectively, and the Habilitation degree from the Bialystok University of Technology, in 2012. Since 1997, he has been with the Faculty of Electrical Engineering, Wrocław University of Technology, where he has been a Professor with the Department of Electrical Engineering, since 2019, and is currently the Head of the Chair of Electrical Engineering Fundamentals. He received the Title of Full Professor from the President of Poland and the President of Czech Republic, in 2019.